

Fig. 3. Transcriptional activation of *IGFBP7* by p53. (A) In silico identification of p53REs. The structure of *IGFBP7* within the genome is shown. The putative p53RE in *IGFBP7* is shown as RE-*IGFBP7*. The nucleotide sequences of conserved p53REs are shown below (consensus). (B) ChIP analysis of *IGFBP7* p53RE. ChIP analysis was carried out using DLD-1 cells transfected with Ad-LacZ or Ad-p53, after which the chromatin was immunoprecipitated with anti-p53 antibody. The DNA was subjected to PCR using primers amplifying the region around RE-*IGFBP7*. (C) Luciferase assay for RE-*IGFBP7*. H1299 cells were cotransfected with empty vector or p53 plus pGL3-RE-*IGFBP7* or pGL3-RE-*IGFBP7*-mut. The relative luciferase activity was defined as the activity in the cells transfected with pGL3-RE-*IGFBP7* divided by the activity in cells transfected with pGL3-RE-*IGFBP7*-mut. (D) Induction of *IGFBP7* by p53. (E) Restoration of p53-induced *IGFBP7* expression by DAC.

When we then used TaqMan real-time reverse transcriptase-PCR to determine the relative levels of *IGFBP7* expression in the same samples, the results were consistent with those summarized above (Figure 1B), which strongly suggests that, in CRC, *IGFBP7* is a frequent target of epigenetic silencing through DNA methylation.

Analysis of *IGFBP7* methylation in CRC cell lines

Because *IGFBP7* contains a CpG island in the region around its transcription start site, we next carried out MSP analysis using the primers illustrated in Figure 2A. We found that *IGFBP7* is completely or strongly methylated in the six CRC cell lines (Colo320, DLD1, HCT116, HT29, RKO and SW48) in which *IGFBP7* is silenced or downregulated (Figure 2B). In addition, detectable but relatively weak methylation was also found in cell lines (CaCO2, LoVo and DKO2) in which *IGFBP7* was expressed and in normal colonic mucosa (Figure 2B).

We verified the MSP results in selected samples using bisulfite sequencing, which revealed that the CpG island of *IGFBP7* is extensively methylated in CRC cell lines in which methylation was detected by MSP (Figure 2C). We also carried out a quantitative analysis of the methylation of six CpG sites located at the core of

the CpG island using primers designed for bisulfite pyrosequencing (Figure 2D and E). The results confirmed the presence of high levels of methylation in cells in which *IGFBP7* expression was silenced or downregulated (DLD1, HCT116, HT29, RKO and SW48). In contrast, methylation levels were lower in cell lines in which *IGFBP7* was expressed (CaCO2, LoVo and SW480). DKO2 cells and normal colonic mucosa also showed low levels of *IGFBP7* methylation. In summary, we observed an inverse correlation between DNA methylation and *IGFBP7* expression in CRC cells.

To confirm that the CpG island is the promoter driving *IGFBP7* expression, we carried out ChIP-PCR to assess trimethylation of H3K4, which is reportedly a marker of active promoters (28). In both DAC-treated HCT116 cells and DKO2 cells, we observed significant enrichment of trimethylated H3K4 in the CpG island. In contrast, very little trimethylated H3K4 was detected in untreated HCT116 cells (Figure 2F).

Identification of *IGFBP7* as a target gene of p53

We previously used a comparative genomic approach in which p53RE was employed as probe to identify novel p53 target genes (14). Using the same in silico analysis in the present study, we found a putative

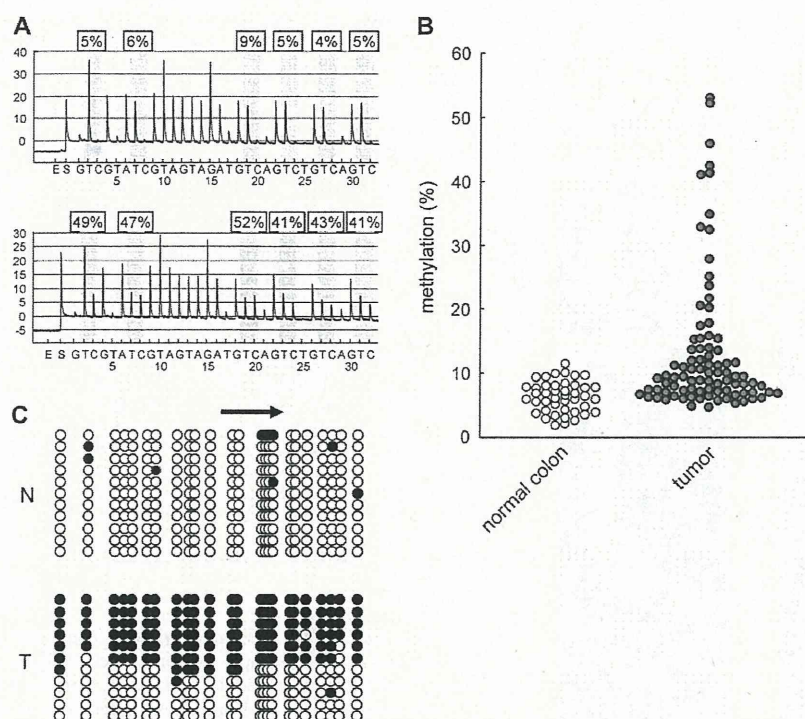


Fig. 4. Analysis of *IGFBP7* methylation in primary colorectal tumors. (A) Representative results of pyrosequencing of *IGFBP7*. (B) Diagram summarizing the levels of *IGFBP7* methylation detected using pyrosequencing. (C) Bisulfite sequencing of *IGFBP7* in primary CRC: Open and filled circles represent unmethylated and methylated CpG sites, respectively: N, normal colon; T, CRC.

p53RE within intron 1 of *IGFBP7* (Figure 3A). p53REs typically consist of two copies of a 10 bp motif (RRRCWWGYYY) separated by 0–12 bp. The putative p53RE for *IGFBP7* (RE-*IGFBP7*) contains a mismatch at a non-critical position within the 20 bp consensus p53-binding sequence (Figure 3A). To determine whether, in fact, p53 directly binds to RE-*IGFBP7*, we carried out ChIP assays using DLD1 cells infected with Ad-p53. After immunoprecipitating DNA–protein complexes from the cross-linked extracts of Ad-p53-infected and control cells using an anti-p53 antibody, we used PCR amplification to measure the abundance of candidate p53REs within the immunoprecipitated complexes. Subsequent ChIP assays confirmed that p53 did indeed bind to DNA fragments containing RE-*IGFBP7* (Figure 3B). To then determine whether p53 can transactivate gene expression via RE-*IGFBP7*, we carried out promoter reporter assays using a luciferase vector containing the wild-type RE-*IGFBP7* sequence upstream of the basal SV40 promoter (pGL3-RE-*IGFBP7*-wt) and a control reporter containing an unresponsive mutated RE-*IGFBP7* sequence (pGL3-RE-*IGFBP7*-mut). H1299 cells, which are null for p53 (29), were transiently cotransfected with one of the reporter plasmids along with a p53 expression vector or an empty vector. In contrast to pGL3-RE-*IGFBP7*-mut, luciferase activity from pGL3-RE-*IGFBP7*-wt was significantly upregulated when cotransfected with a p53 (Figure 3C).

To investigate the effect of p53 on endogenous induction of *IGFBP7*, we assessed expression of *IGFBP7* mRNA in cell lines infected with Ad-p53. Real-time PCR showed that exogenous p53 induced expression of *IGFBP7* mRNA in both H1299 (p53 null, ref. 29) and DLD1 cells (p53 mutant, ref. 30) (Figure 3D). To then assess the role of endogenous p53 in the expression of *IGFBP7*, we treated HCT116 cells with ADR, an agent known to damage DNA and induce endogenous p53 expression, with or without DAC. In a previous study, we showed that ADR, but not DAC, activated p53 and that typical p53 target genes were significantly induced by ADR alone (14,31). However, because *IGFBP7* is methylated and silenced in

HCT116 cells, ADR alone could not induce expression of *IGFBP7* mRNA. In contrast, a low dose of DAC (0.1 μ M) did induce its expression, and we observed further upregulation *IGFBP7* transcription upon addition of ADR (Figure 3E). When we treated p53^{-/-} HCT116 cells with the same low dose of DAC, the induction was quite weak, and no synergistic upregulation was seen upon addition of ADR (Figure 3E).

To determine the extent to which responsiveness to p53 is affected by methylation in the region around the p53REs, we assessed the methylation status of CpG sites in the vicinity of the p53REs. We found that the region around p53REs was methylated regardless of gene expression. Moreover, this region was also methylated in normal tissues, suggesting that methylation of p53REs does not affect the binding of p53 (supplementary Figure 2 is available at *Carcinogenesis* Online). Taken together, these observations support the idea that *IGFBP7* is a direct target of p53, and its induction can be blocked by DNA hypermethylation.

Growth suppressive effect of *IGFBP7*

To test whether *IGFBP7* suppresses CRC cell growth, we cloned the full-length *IGFBP7* cDNA into pcDNA3.1 vector, after which we transfected HCT116 cells with the resultant pcDNA3.1His-*IGFBP7* vector and verified secretion of the expressed *IGFBP7* protein into the conditioned medium (supplementary Figure 1A is available at *Carcinogenesis* Online). We then tested the transfectants in colony formation assays and found that overexpression of *IGFBP7* markedly suppressed colony formation (supplementary Figure 1B and C is available at *Carcinogenesis* Online).

Correlation between *IGFBP7* methylation and other epigenetic/genetic alterations in CRC and adenoma

We next analyzed the methylation of the *IGFBP7* CpG island in a panel of tumor specimens from CRC patients. Because MSP



Fig. 5. Epigenetic and genetic alterations in CRCs (A) and colorectal adenomas (B). K-means clustering analysis based on epigenetic and genetic alterations. Each column represents the separate gene locus shown on the top. Each row is a primary CRC or adenoma: red rectangles, methylated/mutated tumors; green rectangles, unmethylated/wild-type tumors. Fifteen percent methylation was used as the cutoff criterion for methylation of *IGFBP7*.

revealed a low level of *IGFBP7* methylation in normal colonic mucosa, we carried out bisulfite pyrosequencing to quantitatively analyze *IGFBP7* methylation (Figure 4A). As summarized in Figure 4B, levels of *IGFBP7* methylation were significantly higher in primary tumors than in normal colonic tissue ($P < 0.001$). We confirmed these results with bisulfite sequencing in selected specimens. In normal colonic tissue, the vast majority of the CpG island was unmethylated (Figure 4C). On the other hand, tumor tissue in which elevated methylation was detected showed a mixture of entirely and partially

Table I. Correlation between methylation of *IGFBP7* and other epigenetic and genetic alterations

		IGFBP7 methylation		
		Mean values	SD	<i>P</i>
Age		$R = 0.117$		0.292
Sex		14.3	13.2	0.563
	F (25)	12.8	9.4	
	M (58)	21.4	15.1	
p16	Unmethylated (60)	10.2	6.1	0.002
	Methylated (23)	21.4	15.1	
hMLH1	Unmethylated (67)	9.7	4.5	<0.001
	Methylated (16)	28.4	15.0	
K-ras	Wild-type (45)	16.7	13.1	0.001
	Mutated (38)	9.2	3.7	
BRAF	Wild-type (75)	11.0	7.3	0.001
	Mutated (8)	35.2	12.5	
p53	Wild-type (44)	16.4	13.1	0.003
	Mutated (39)	9.8	5.0	
MSI	Stable (66)	9.7	4.5	<0.001
	Unstable (17)	27.2	15.3	
CIMP	Absent (42)	9.6	4.8	0.002
	Present (41)	17.0	13.4	

methylated alleles and unmethylated alleles, probably reflecting contamination of the sample by normal cells (Figure 5C).

Finally, we examined the correlation between *IGFBP7* methylation and other genetic and epigenetic alterations in CRCs (Figure 5A, Table I). We found that there are significant correlations between levels of *IGFBP7* methylation and methylation of *p16* ($P < 0.001$) and *hMLH1* ($P < 0.001$), mutation of *BRAF* ($P < 0.001$), CIMP ($P = 0.002$) and microsatellite instability ($P < 0.001$). Levels of *IGFBP7* methylation were inversely correlated with mutation of *K-ras* ($P = 0.001$) and *p53* ($P = 0.014$). Of 49 colorectal adenomas, nine (18%) showed *IGFBP7* methylation and three (6%) showed *BRAF* mutation, while none showed *hMLH1* methylation or microsatellite instability, indicating that inactivation of *IGFBP7* is an early event in colorectal tumorigenesis (Figure 5B).

Discussion

A subset of CRCs show methylation of multiple CpG islands, indicating that these tumors have CIMP (5). CRCs with CIMP are closely associated with microsatellite instability through methylation of *hMLH1* (5) and frequently show *BRAF* mutations (8), which indicates that these tumors arise via distinct pathways that differ from classical multistep tumorigenesis (6). In the present study, we found that methylation of *IGFBP7* is strongly associated with *BRAF* mutation and the presence of CIMP. Moreover, the earlier finding that *BRAF* mutations are common in hyperplastic polyps and serrated adenomas suggests CRCs with CIMP/*IGFBP7* methylation arise via the serrated pathway (32). It is also known that Ras-mediated epigenetic silencing of effectors, including DNMT1, plays a key role in cellular transformation (33) and that DNMT1 is a downstream target of the Ras-signaling pathway (34). This suggests that *BRAF* activation may be involved in the CIMP phenotype through activation of the DNA methylation machinery. Because the colorectal adenomas examined in this study were not serrated adenomas, further study will be necessary to determine the incidence of *IGFBP7* methylation among serrated adenomas.

It remains unclear why CIMP is associated with *BRAF* mutation. Mutations leading to *BRAF* activation are found in several types of human tumors. Substituting a glutamic acid for a valine at position 600 (BRAFV600E) substantially increases BRAF's protein kinase activity, leading to constitutive extracellular signal-regulated kinase signaling (35,36). However, activation of BRAFV600E does not fully transform primary human cells, indicating that additional cooperative events are required for tumorigenesis (37). Indeed, expression of BRAFV600E induces senescence in cultured primary human

melanocytes (37). And although BRAF mutations are frequently seen in colorectal hyperplastic polyps, these tumors undergo senescence (38). It has therefore been speculated that genes involved in the induction of senescence by BRAF are altered during the progression of tumors. In addition, IGFBP7 was recently shown to play an important role in Ras-mediated senescence (19). Our results thus suggest that CRCs with CIMP may escape senescence by both activating oncogenic signaling (e.g. BRAF mutations) and inactivating regulators of senescence (e.g. IGFBP7 methylation).

The regulatory mechanisms controlling IGFBP7 expression are not fully understood. p53 is a transcription factor that activates expression of genes involved in cell cycle checkpoints, apoptosis and DNA repair (39). Although CRCs with CIMP show only a low frequency of p53 mutations, the function of p53 may nonetheless be impaired in these tumors due to epigenetic inactivation of target genes, including IGFBP7 family members such as IGFBP7 and IGFBP3 (40). Consistent with that idea, several targets of p53 are known to be silenced by DNA methylation (20,41,42). In the present study, we found that IGFBP7 is not expressed in HCT116 cells but that expression could be restored by treating the cells with DAC. Moreover, Ad-p53 acts synergistically with DAC to further upregulate IGFBP7 expression. These findings suggest that combining a DNA methyltransferase inhibitor with drugs that induce p53-dependent growth inhibition may be a useful approach to treating CRC. In fact, Lin *et al.* (43) recently reported that reactivation of IGFBP7 using DAC inhibits CRC cell growth.

Weak methylation of IGFBP7 was even detected in DKO2 cells. Although DKO2 cells lack both DNMT1 and DNMT3B, this cell line does express a different DNA methyltransferase, DNMT3A, which may maintain the observed methylation. Alternatively, residual activity of truncated DNMT1 may be sufficient to maintain the low level of IGFBP7 methylation seen in DKO2 cells (44). In addition, expression of IGFBP7 was not fully restored by DAC treatment in HT29 and RKO cells (Figure 1B), which suggests that other cofactors involved in induction of IGFBP7 also may be impaired in these cell lines.

The molecular mechanism by which IGFBP7 contributes to tumor suppression is not fully understood, though IGFBP7 has been shown to suppress cell growth and induce apoptosis (45,46). In lung and prostate cancers, for example, IGFBP7 induces apoptosis by upregulating expression of Caspase-3 (47,48). On the other hand, knocking down IGFBP7 had no effect on cell growth *in vitro*, though IGFBP7 did suppress anchorage-independent and *in vivo* cell growth (49), suggesting that the effects of IGFBP7 on cell growth vary depending upon the cell type. IGFBP7 is a cell adhesion factor that promotes cell adhesion by binding to cell surface heparin sulfate proteoglycans (50,51). Because CRCs showing expression of IGFBP7 do not grow *in vivo*, Sato *et al.* (49) proposed that although IGFBP7 is involved in cell adhesion, it suppresses anchorage-dependent cell growth *in vivo*. Further study will be necessary to clarify the mechanism by which IGFBP7 modulates growth signaling pathways to suppress the growth of cancer cells.

In summary, we found that IGFBP7 is a direct target of p53, indicating that IGFBP7 is a mediator of p53-dependent growth suppression. DAC and Ad-p53 acted synergistically to induce IGFBP7 expression in CRC cells where it was otherwise silenced by methylation. We also found that IGFBP7 methylation is associated with the BRAF mutations, the absence of p53 mutations and the presence of CIMP in CRCs. Thus, epigenetic inactivation of IGFBP7 appears to be a potentially useful molecular target for the diagnosis and treatment of CRCs with CIMP.

Supplementary material

Supplementary Figures 1 and 2 and Table 1 can be found at <http://carcin.oxfordjournals.org/>

Funding

Grants-in-Aid for Scientific Research on Priority Areas from the Ministry of Education, Culture, Sports, Science and Technology (K.I., T.T.

and M.T.); Grants-in-Aid for Scientific Research (S) from Japan Society for Promotion of Science (K.I.); Grant-in-Aid for the Third-term Comprehensive 10 year Strategy for Cancer Control; Grant-in-Aid for Cancer Research from the Ministry of Health, Labor, and Welfare, Japan (M.T.).

Acknowledgements

The authors thank Dr William F. Goldman for editing the manuscript.

Conflict of Interest Statement: None declared.

References

- Kinzler, K.W. *et al.* (1996) Lessons from hereditary colorectal cancer. *Cell*, **87**, 159–170.
- Jones, P.A. *et al.* (2007) The epigenomics of cancer. *Cell*, **128**, 683–692.
- Kanai, Y. *et al.* (2007) Alterations of DNA methylation associated with abnormalities of DNA methyltransferases in human cancers during transition from a precancerous to a malignant state. *Carcinogenesis*, **28**, 2434–2442.
- Ushijima, T. *et al.* (2005) Aberrant methylations in cancer cells: where do they come from? *Cancer Sci.*, **96**, 206–211.
- Toyota, M. *et al.* (1999) CpG island methylator phenotype in colorectal cancer. *Proc. Natl Acad. Sci. USA*, **96**, 8681–8686.
- Shen, L. *et al.* (2007) Integrated genetic and epigenetic analysis identifies three different subclasses of colon cancer. *Proc. Natl Acad. Sci. USA*, **104**, 18654–18659.
- Toyota, M. *et al.* (2000) Distinct genetic profiles in colorectal tumors with or without the CpG island methylator phenotype. *Proc. Natl Acad. Sci. USA*, **97**, 710–715.
- Weisenberger, D.J. *et al.* (2006) CpG island methylator phenotype underlies sporadic microsatellite instability and is tightly associated with BRAF mutation in colorectal cancer. *Nat. Genet.*, **38**, 787–793.
- Serrano, M. *et al.* (1997) Oncogenic ras provokes premature cell senescence associated with accumulation of p53 and p16INK4a. *Cell*, **88**, 593–602.
- Zhu, J. *et al.* (1998) Senescence of human fibroblasts induced by oncogenic Raf. *Genes Dev.*, **12**, 2997–3007.
- Kortlever, R.M. *et al.* (2006) Plasminogen activator inhibitor-1 is a critical downstream target of p53 in the induction of replicative senescence. *Nat. Cell Biol.*, **8**, 877–884.
- Qian, Y. *et al.* (2008) DEC1, a basic helix-loop-helix transcription factor and a novel target gene of the p53 family, mediates p53-dependent premature senescence. *J. Biol. Chem.*, **283**, 2896–2905.
- el-Deiry, W.S. (1998) Regulation of p53 downstream genes. *Semin. Cancer Biol.*, **8**, 345–357.
- Maruyama, R. *et al.* (2006) Comparative genome analysis identifies the vitamin D receptor gene as a direct target of p53-mediated transcriptional activation. *Cancer Res.*, **66**, 4574–4583.
- Burger, A.M. *et al.* (1998) Down-regulation of T1A12/mac25, a novel insulin-like growth factor binding protein related gene, is associated with disease progression in breast carcinomas. *Oncogene*, **16**, 2459–2467.
- Landberg, G. *et al.* (2001) Downregulation of the potential suppressor gene IGFBP-rP1 in human breast cancer is associated with inactivation of the retinoblastoma protein, cyclin E overexpression and increased proliferation in estrogen receptor negative tumors. *Oncogene*, **20**, 3497–3505.
- Lin, J. *et al.* (2007) Methylation patterns of IGFBP7 in colon cancer cell lines are associated with levels of gene expression. *J. Pathol.*, **212**, 83–90.
- Yamashita, S. *et al.* (2006) Chemical genomic screening for methylation-silenced genes in gastric cancer cell lines using 5-aza-2'-deoxycytidine treatment and oligonucleotide microarray. *Cancer Sci.*, **97**, 64–71.
- Wajapeyee, N. *et al.* (2008) Oncogenic BRAF induces senescence and apoptosis through pathways mediated by the secreted protein IGFBP7. *Cell*, **132**, 363–374.
- Toyota, M. *et al.* (2008) Epigenetic silencing of microRNA-34b/c and B-cell translocation gene 4 is associated with CpG island methylation in colorectal cancer. *Cancer Res.*, **68**, 4123–4132.
- Rhee, I. *et al.* (2002) DNMT1 and DNMT3b cooperate to silence genes in human cancer cells. *Nature*, **416**, 552–556.
- Bunz, F. *et al.* (1998) Requirement for p53 and p21 to sustain G2 arrest after DNA damage. *Science*, **282**, 1497–1501.
- Herman, J.G. *et al.* (1996) Methylation-specific PCR: a novel PCR assay for methylation status of CpG islands. *Proc. Natl Acad. Sci. USA*, **93**, 9821–9826.

24. Sasaki, Y. *et al.* (2003) Identification of the interleukin 4 receptor alpha gene as a direct target for p73. *Cancer Res.*, **63**, 8145–8152.
25. Nojima, M. *et al.* (2007) Frequent epigenetic inactivation of SFRP genes and constitutive activation of Wnt signaling in gastric cancer. *Oncogene*, **26**, 4699–4713.
26. Akino, K. *et al.* (2005) The Ras effector RASSF2 is a novel tumor-suppressor gene in human colorectal cancer. *Gastroenterology*, **129**, 156–169.
27. Eisen, M.B. *et al.* (1998) Cluster analysis and display of genome-wide expression patterns. *Proc. Natl Acad. Sci. USA*, **95**, 14863–14868.
28. Barski, A. *et al.* (2007) High-resolution profiling of histone methylations in the human genome. *Cell*, **129**, 823–837.
29. Chen, J.Y. *et al.* (1993) Heterogeneity of transcriptional activity of mutant p53 proteins and p53 DNA target sequences. *Oncogene*, **8**, 2159–2166.
30. Yu, J. *et al.* (1999) Identification and classification of p53-regulated genes. *Proc. Natl Acad. Sci. USA*, **96**, 14517–14522.
31. Adachi, K. *et al.* (2004) Identification of SCN3B as a novel p53-inducible proapoptotic gene. *Oncogene*, **23**, 7791–7798.
32. Minoo, P. *et al.* (2007) Prognostic significance of mammalian sterile20-like kinase 1 in colorectal cancer. *Mod. Pathol.*, **20**, 331–338.
33. Gazin, C. *et al.* (2007) An elaborate pathway required for Ras-mediated epigenetic silencing. *Nature*, **449**, 1073–1077.
34. Bakin, A.V. *et al.* (1999) Role of DNA 5-methylcytosine transferase in cell transformation by fos. *Science*, **283**, 387–390.
35. Davies, H. *et al.* (2002) Mutations of the BRAF gene in human cancer. *Nature*, **417**, 949–954.
36. Rajagopalan, H. *et al.* (2002) Tumorigenesis: RAF/RAS oncogenes and mismatch-repair status. *Nature*, **418**, 934.
37. Michaloglou, C. *et al.* (2005) BRAFE600-associated senescence-like cell cycle arrest of human naevi. *Nature*, **436**, 720–724.
38. Minoo, P. *et al.* (2006) Senescence and serration: a new twist to an old tale. *J. Pathol.*, **210**, 137–140.
39. Riley, T. *et al.* (2008) Transcriptional control of human p53-regulated genes. *Nat. Rev. Mol. Cell Biol.*, **9**, 402–412.
40. Buckbinder, L. *et al.* (1995) Induction of the growth inhibitor IGF-binding protein 3 by p53. *Nature*, **377**, 646–649.
41. Suzuki, H. *et al.* (2000) Inactivation of the 14-3-3 sigma gene is associated with 5' CpG island hypermethylation in human cancers. *Cancer Res.*, **60**, 4353–4357.
42. Wales, M.M. *et al.* (1995) p53 activates expression of HIC-1, a new candidate tumour suppressor gene on 17p13.3. *Nat. Med.*, **1**, 570–577.
43. Lin, J. *et al.* (2008) Reactivation of IGFBP7 by DNA demethylation inhibits human colon cancer cell growth *in vitro*. *Cancer Biol. Ther.*, **7**, 1896–1900.
44. Egger, G. *et al.* (2006) Identification of DNMT1 (DNA methyltransferase 1) hypomorphs in somatic knockouts suggests an essential role for DNMT1 in cell survival. *Proc. Natl Acad. Sci. USA*, **103**, 14080–14085.
45. Sprenger, C.C. *et al.* (2002) Over-expression of insulin-like growth factor binding protein-related protein-1(IGFBP-rP1/mac25) in the M12 prostate cancer cell line alters tumor growth by a delay in G1 and cyclin A associated apoptosis. *Oncogene*, **21**, 140–147.
46. Wilson, H.M. *et al.* (2002) Insulin-like growth factor binding protein-related protein 1 inhibits proliferation of MCF-7 breast cancer cells via a senescence-like mechanism. *Cell Growth Differ.*, **13**, 205–213.
47. Chen, Y. *et al.* (2007) Insulin-like growth factor binding protein-related protein 1 (IGFBP-rP1) has potential tumour-suppressive activity in human lung cancer. *J. Pathol.*, **211**, 431–438.
48. Mutaguchi, K. *et al.* (2003) Restoration of insulin-like growth factor binding protein-related protein 1 has a tumor-suppressive activity through induction of apoptosis in human prostate cancer. *Cancer Res.*, **63**, 7717–7723.
49. Sato, Y. *et al.* (2007) Strong suppression of tumor growth by insulin-like growth factor-binding protein-related protein 1/tumor-derived cell adhesion factor/mac25. *Cancer Sci.*, **98**, 1055–1063.
50. Akaogi, K. *et al.* (1994) Cell adhesion activity of a 30-kDa major secreted protein from human bladder carcinoma cells. *Biochem. Biophys. Res. Commun.*, **198**, 1046–1053.
51. Sato, J. *et al.* (1999) Identification of cell-binding site of angiomodulin (AGM/TAF/Mac25) that interacts with heparan sulfates on cell surface. *J. Cell. Biochem.*, **75**, 187–195.

Received March 7, 2009; revised June 21, 2009; accepted July 17, 2009

Methylation-associated silencing of microRNA-34b/c in gastric cancer and its involvement in an epigenetic field defect

Hiromu Suzuki^{1,2,†}, Eiichiro Yamamoto^{1,2,†},
Masanori Nojima^{1,3}, Masahiro Kai², Hiro-o Yamano⁴,
Kenjiro Yoshikawa⁴, Tomoaki Kimura⁴, Toyoki Kudo⁴,
Eiji Harada⁴, Tamotsu Sugai⁵, Hiroyuki Takamaru¹,
Takeshi Niinuma¹, Reo Maruyama¹, Hiroyuki Yamamoto¹,
Takashi Tokino⁶, Kohzoh Imai⁷, Minoru Toyota² and
Yasuhisa Shinomura^{1,*}

¹First Department of Internal Medicine, Sapporo Medical University, S1, W16, Chuo-Ku, Sapporo 064-8543, Japan, ²Department of Biochemistry and ³Department of Public Health, Sapporo Medical University, Sapporo 060-8556, Japan, ⁴Department of Gastroenterology, Akita Red Cross Hospital, Akita 010-1495, Japan, ⁵Division of Diagnostic Molecular Pathology, Department of Pathology, Iwate Medical University, Morioka 020-8505, Japan, ⁶Department of Molecular Biology, Cancer Research Institute, Sapporo Medical University, Sapporo 060-8556, Japan and ⁷Division of Oncology, The Advanced Clinical Research Center, The Institute of Medical Science, The University of Tokyo, Tokyo 108-1639, Japan

*To whom correspondence should be addressed. Tel: +81 11 611 2111; Fax: +81 11 611 2282; Email: shinomura@sapmed.ac.jp
Correspondence may also be addressed to Minoru Toyota. Department of Biochemistry, Sapporo Medical University, S1, W17, Chuo-Ku, Sapporo 060-8556, Japan. Tel: +81 11 611 2111; Fax: +81 11 611 2282; Email: mtoyota@sapmed.ac.jp

Altered expression of microRNA (miRNA) is strongly implicated in cancer, and recent studies have shown that the silencing of some miRNAs is associated with CpG island hypermethylation. To identify epigenetically silenced miRNAs in gastric cancer (GC), we screened for miRNAs induced by treatment with 5-aza-2'-deoxycytidine and 4-phenylbutyrate. We found that *miR-34b* and *miR-34c* are epigenetically silenced in GC and that their downregulation is associated with hypermethylation of the neighboring CpG island. Methylation of the *miR-34b/c* CpG island was frequently observed in GC cell lines (13/13, 100%) but not in normal gastric mucosa from *Helicobacter pylori*-negative healthy individuals. Transfection of a precursor of *miR-34b* and *miR-34c* into GC cells induced growth suppression and dramatically changed the gene expression profile. Methylation of *miR-34b/c* was found in a majority of primary GC specimens (83/118, 70%). Notably, analysis of non-cancerous gastric mucosae from GC patients ($n = 109$) and healthy individuals ($n = 85$) revealed that methylation levels are higher in gastric mucosae from patients with multiple GC than in mucosae from patients with single GC (27.3 versus 20.8%; $P < 0.001$) or mucosae from *H. pylori*-positive healthy individuals (27.3 versus 20.7%; $P < 0.001$). These results suggest that *miR-34b* and *miR-34c* are novel tumor suppressors frequently silenced by DNA methylation in GC, that methylation of *miR-34b/c* is involved in an epigenetic field defect and that the methylation might be a predictive marker of GC risk.

Introduction

MicroRNAs (miRNAs) are small non-coding RNAs that regulate gene expression by inducing degradation or translational inhibition of partially complementary target messenger RNAs. The ~1000 miRNAs

Abbreviations: DAC, 5-aza-2'-deoxycytidine; DNMT, DNA methyltransferase; GC, gastric cancer; mAb, monoclonal antibody; miRNA, microRNA; OR, odds ratio; PBA, 4-phenylbutyrate; PCR, polymerase chain reaction; RT-PCR, reverse transcription-polymerase chain reaction.

[†]These authors contributed equally to this work.

thought to be encoded in the human genome play pivotal roles in a wide array of biological processes, including cell proliferation and differentiation and apoptosis (1,2). In recent years, a number of studies have provided evidence that dysregulation of miRNA expression contributes to the initiation and progression of human cancer (1,2). Indeed, downregulation of a subset of miRNAs is a commonly observed feature of cancers, suggesting that these molecules may act as tumor suppressors (3). The first report of altered miRNA expression in cancer was the frequent chromosomal deletion and downregulated expression of *miR-15* and *miR-16*, two miRNAs thought to target the antiapoptotic factor BCL2, in chronic lymphocytic leukemia (4). Another example is let-7, which negatively regulates expression of Ras oncogenes (5); its downregulation in tumors is thought to contribute to activation of the Ras signaling pathway.

Although the mechanism underlying miRNA dysregulation in cancer is not yet fully understood, recent studies have shown that the silencing of several miRNAs is tightly linked to epigenetic mechanisms, such as histone modification and DNA methylation. It was shown, for example, that pharmacological unmasking of silenced genes using histone deacetylase and DNA methyltransferase (DNMT) inhibitors restored *miR-127* expression in a human bladder cancer cell line (6) and that genetic disruption of DNMTs restored expression of *miR-124a* in a colorectal cancer cell line (7). Notably, the DNA sequences encoding *miR-127* and *miR-124a* are embedded within CpG islands that are hypermethylated in cancer cells. Similarly, we found that the frequent silencing of *miR-34b* and *miR-34c* in colorectal cancer is associated with CpG island hypermethylation (8). Taken together, these results suggest that, as with other tumor suppressor genes, DNA methylation is a major mechanism by which miRNA expression is silenced in cancer.

Gastric cancer (GC) is one of the most common causes of death from cancer among both men and women around the world (9). To date, we and many others have identified a wide variety of tumor suppressor genes and other tumor-related genes that are inactivated by aberrant DNA methylation in GC (10–12). Moreover, it was recently shown that epigenetic mechanisms are involved in the alteration of several miRNA genes in GC (13,14), though much remains to be learned about the dysregulation of miRNAs in this disease. In the present study, we aimed to identify miRNAs whose expression is epigenetically silenced in GC by screening for miRNAs whose expression is upregulated by DNA demethylation and histone deacetylase inhibition in GC cell lines. We found that *miR-34b* and *miR-34c* are frequent targets of epigenetic silencing in GC, and analysis in primary GC and non-cancerous gastric mucosa specimens revealed a significant involvement of *miR-34b/c* methylation in the development of an epigenetic field defect during stomach carcinogenesis.

Materials and methods

Cell lines and tissues

GC cell lines (MKN74, SNU1, SNU638, JRST, KatoIII, AZ521, MKN28, MKN45, NUGC3, NUGC4, AGS and NCI-N87) were obtained and cultured as described previously (15). SH101 cells were kindly provided by Dr K. Yanagihara at the National Cancer Research Institute and were described previously (16). To analyze restoration of silenced genes, cells were treated with 5-aza-2'-deoxycytidine (DAC; Sigma-Aldrich, St Louis, MO) or with a combination of DAC and 4-phenylbutyrate (PBA; Sigma-Aldrich). Cells were treated with 2 μ M DAC for 72 h, replacing the drug and medium every 24 h. In the combined protocol, cells (MKN74 and AGS) were treated first with 2 μ M DAC for 72 h and then with 3 mM PBA for an additional 72 h, replacing the drug and medium every 24 h. A total of 118 primary GC specimens were obtained from surgical resection (15,17) or endoscopic biopsy (82 male and 36 female; average age 66 years, ranging from 36 to 89). Non-cancerous gastric mucosae were obtained by endoscopic biopsy from 109 well-differentiated GC patients (82 male and 27 female; average age 69 years, ranging from 35 to 89).

Normal gastric mucosae were also obtained by endoscopic biopsy from 85 healthy individuals (61 male and 24 female; average age 58 years, ranging from 22 to 89). Biopsies of non-cancerous gastric mucosa or normal gastric mucosa were obtained from two independent sites (gastric body and antrum) in each individual. *Helicobacter pylori* infection was identified using a rapid urease test, a serum antibody test or a urea breath test. The updated Sydney System was used to estimate the degree of gastritis (18). Informed consent was obtained from all patients before collecting the specimens. Genomic DNA was extracted using the standard phenol–chloroform procedure. Total RNA was extracted using TRIZOL reagent (Invitrogen, Carlsbad, CA) and then treated with a DNA-free kit (Ambion, Austin, TX). Genomic DNA and total RNA from normal gastric mucosa from a healthy individual were purchased from BioChain (Hayward, CA).

miRNA microarray analysis

miRNA expression was analyzed using a color microarray according to the manufacturer's instructions (Agilent Technologies, Santa Clara, CA). Briefly, 100 ng of total RNA was amplified and labeled using a miRNA Labeling Reagent (Agilent Technologies), after which the labeled RNA was hybridized to a human miRNA microarray (G4470A; Agilent technologies). Once hybridized, the array was scanned using an Agilent DNA Microarray Scanner (Agilent technologies), and the data were processed using Feature Extraction software (Agilent technologies). The data were then further analyzed using GeneSpring GX version 10 (Agilent technologies).

Real-time reverse transcription–polymerase chain reaction of miRNA

Expression of mature *miR-34b/c* was analyzed using TaqMan MicroRNA Assays (Applied Biosystems, Foster City, CA). Briefly, 5 ng of small RNA or total RNA was reverse transcribed using specific stem–loop reverse transcription primers, after which they were amplified and detected using polymerase chain reaction (PCR) with specific primers and TaqMan probes. The PCR was run in a 7900HT Fast Real-Time PCR System (Applied Biosystems), and SDS2.2.2 software (Applied Biosystems) was used for comparative delta Ct analysis. U6 snoRNA (RNU6B; Applied Biosystems) served as an endogenous control.

Promoter assay

A pGL3 vector harboring the *miR-34b/c* promoter region was prepared as described previously (8). Cells (5×10^4 cells per well in 24-well plates) were transfected with 100 ng of one of the reporter plasmids and 2 ng of pRL-TK (Promega, Madison, WI) using Lipofectamine 2000 (Invitrogen). Luciferase activities were then measured 48 h after transfection using a Dual-Luciferase Reporter Assay System (Promega).

Methylation analysis

Genomic DNA (2 μ g) was modified with sodium bisulfite using an EpiTect Bisulfite Kit (Qiagen, Hilden, Germany). *In vitro* methylated DNA served as a positive control for DNA methylation, as described previously (8). Genomic DNA from a colon cancer cell line HCT116 harboring genetic disruptions within the *DNMT1* and *DNMT3B* loci (DNMTs KO) served as a negative control (8). Methylation-specific PCR, bisulfite sequencing and bisulfite pyrosequencing were carried out as described previously (8,15). For bisulfite sequencing analysis, amplified PCR products were cloned into pCR2.1-TOPO vector (Invitrogen), and 10–12 clones from each sample were sequenced using an ABI3130x automated sequencer (Applied Biosystems). For bisulfite pyrosequencing, the biotinylated PCR product was purified, made single-stranded and used as a template in a pyrosequencing reaction run according to the manufacturer's instructions. The PCR products were bound to streptavidin sepharose beads HP (Amersham Biosciences, Piscataway, NJ), after which beads containing the immobilized PCR product were purified, washed and denatured using a 0.2 M NaOH solution. After addition of 0.3 μ M sequencing primer to the purified PCR product, pyrosequencing was carried out using a PSQ96MA system (Biotage, Uppsala, Sweden) and Pyro Q-CpG software (Biotage). Primer sequences and PCR product sizes are listed in supplementary Table 1 (available at *Carcinogenesis* Online).

Transfection of precursor miRNA

Cells (5×10^6 cells) were transfected with 100 pmol of Pre-miR miRNA Precursor Molecules (Ambion) or Pre-miR miRNA Molecules Negative Control #1 (Ambion) using a Cell Line Nucleofector kit V (Amatax, Gaithersburg, MD) with a Nucleofector I electroporation device (Amatax) according to the manufacturer's instructions. Total RNA or cell lysate was extracted 48 h after transfection.

Real-time reverse transcription–polymerase chain reaction

Real-time reverse transcription–polymerase chain reaction (RT–PCR) was carried out using TaqMan Gene Expression Assays (MET, Hs00179845_m1; CDK4, Hs00364847_m1; CCNE2, Hs00180319_m1; CCNA2, Hs00153138_m1;

18S ribosomal RNA, Hs99999901_s1; Applied Biosystems) and a 7500 Fast Real-Time PCR System (Applied Biosystems) according to the manufacturer's instructions. SDS2.2.2 software (Applied Biosystems) was used for comparative delta Ct analysis, and 18S ribosomal RNA (Applied Biosystems) served as an endogenous control.

Gene expression microarray analysis

Total RNA was extracted using TRIZOL (Invitrogen) and then cleaned up using an RNeasy Mini Elute Cleanup kit (Qiagen). Thereafter, one-color microarray-based gene expression analysis was carried out according to the manufacturer's instructions (Agilent Technologies). Briefly, 700 ng of total RNA was amplified and labeled using a Low RNA Input Linear Amplification kit (Agilent Technologies), after which the synthesized complementary RNA was hybridized to the Whole Human Genome Oligo DNA microarray (G4112F; Agilent technologies). Once hybridized, the array was scanned with an Agilent DNA Microarray Scanner (Agilent technologies), and the microarray data were processed using Feature Extraction software (Agilent technologies). For hierarchical clustering analysis, gene ontology and pathway analyses were carried out using GeneSpring GX version 11 (Agilent technologies).

Western blot analysis

Western blot analysis was carried out as described previously (8). Mouse anti-MET (hepatocyte growth factor receptor) monoclonal antibody (mAb) (25H2; Cell Signaling Technology, Danvers, MA), mouse anti-CDK4 mAb (DCS-35; Santa Cruz Biotechnology, Santa Cruz, CA), mouse anti-cyclin E1 mAb (clone EP435E; Millipore, Billerica, MA), rabbit anti-cyclin A2 polyclonal Ab (C-19; Santa Cruz Biotechnology) and mouse anti-actin mAb (Chemicon, Temecula, CA) were all used in accordance with the manufacturer's instructions. The immunoreactive bands were visualized using peroxidase-conjugated anti-mouse IgG antibody (Jackson ImmunoResearch Laboratories, West Grove, PA) and ECL (GE Healthcare Bio-Sciences KK, Tokyo, Japan).

Detection of miRNA by *in situ* hybridization assay

In situ detection of miRNA expression was accomplished using formalin-fixed paraffin-embedded tissue sections. Slides were deparaffinized in a xylene series and then rehydrated through an ethanol series. After deparaffinization, the specimens were digested for 30 min using a DIGEST-ALL 3 kit (Invitrogen). The slides were then hybridized overnight with a LNA-modified digoxigenin-labeled probe (Exiqon, Vedbaek, Denmark) in hybridization solution containing 50% formamide, 2 \times standard saline citrate and 20% dextran sulfate. After stringently washing the slides, Cy3-tyramide signal amplification was carried out, and the signal was detected using a horseradish peroxidase-conjugated antidigoxigenin antibody. Signals were visualized using an AQUA microscope system (HistoRx, New Haven, CT).

Statistical analysis

Statistical analyses were carried out using SPSSJ 15.0 (SPSS Japan Inc., Tokyo, Japan). Levels of *miR-34b/c* methylation were compared among groups using analysis of variance or analysis of covariance (for age-adjusted data), followed by *post hoc* multiple comparison with Sidak correction. Receiver operator characteristic curves were constructed based on the levels of *miR-34b/c* methylation. After categorizing the methylation levels into four quartiles, odds ratios (ORs) for cancer risk or multiple cancer risk were calculated using logistic regression models. Values of $P < 0.05$ (two-sided) were considered significant.

Results

Screening for epigenetically silenced miRNAs in GC cells

To screen for epigenetically silenced miRNAs, we initially carried out miRNA microarray analyses using two GC cell lines (MKN74 and AGS), with or without DAC treatment. In addition, because previous studies have shown that treatment with a combination of DAC and PBA induces stronger reexpression of miRNAs than either agent alone (6,14), GC cells treated with DAC and PBA were also subjected to microarray analysis. We found that the combination treatment induced greater numbers of miRNAs than treatment with DAC alone. Of the 470 miRNAs analyzed in AGS cells, 48 were upregulated (>5-fold) by DAC alone, whereas 135 were upregulated by the combination treatment (supplementary Tables 2 and 3 and Figure 1 are available at *Carcinogenesis* Online). In MKN74 cells, DAC induced upregulation (>5-fold) of 53 miRNAs, whereas the combination treatment upregulated 150 miRNAs (supplementary Tables 4 and 5 and Figure 1 are available at *Carcinogenesis* Online). The majority of the miRNAs showing the strongest upregulation were located in the

miRNA cluster on chromosome 19 (C19MC) (supplementary Table 6 is available at *Carcinogenesis* Online). That this finding is consistent with recent reports validates our drug treatment protocol as well as the findings of the microarray analysis (14,19).

Analysis of miR-34b/c expression in GC cells

Among the miRNAs detected in the microarray analysis, we focused on *miR-34b* and *miR-34c* because *miR-34s* have been strongly implicated in cancer. All three members of *miR-34* family are directly regulated by p53 (20,21) and exhibit tumor suppressive effects in human cancer (8,22). Our microarray analysis revealed that both *miR-34b* and *miR-34c* are upregulated by DAC in MKN74 and AGS cells, whereas *miR-34a* was abundantly expressed in both cell lines, with or without DAC treatment. Moreover, the upregulation of *miR-34b* and *miR-34c* was further enhanced by the combined treatment with DAC and PBA in both cell types.

We next used TaqMan RT-PCR to analyze the expression of *miR-34b/c* in a panel of GC cell lines and in normal stomach tissue. Both *miR-34b* and *miR-34c* were downregulated in all GC cell lines, as compared with normal stomach tissue (Figure 1A), but DAC treatment restored expression of *miR-34b* and *miR-34c* in the GC cells (Figure 1B). We also confirmed that combined treatment with DAC and PBA synergistically upregulated expression of *miR-34b* and

miR-34c in MKN74 and AGS cells (Figure 1C). Thus, *miR-34b* and *miR-34c* appears to be epigenetically silenced in GC.

DNA methylation of the miR-34b/c CpG island in GC cells

It was previously reported that mature *miR-34b* and *miR-34c* are processed from a single primary transcript, and a CpG island in the proximal upstream region of *miR-34b* contains promoter activity (Figure 2A) (8,20). To confirm that finding, we carried out luciferase assays using a reporter construct containing the *miR-34b/c* CpG island and observed high levels of luciferase activity following transient transfection of two GC cell lines (MKN74 and AGS) with the reporter vector (supplementary Figure 2 is available at *Carcinogenesis* Online). We next asked whether DNA methylation in this region is responsible for the silencing of *miR-34b/c* in GC cells. Methylation-specific PCR analysis showed that the CpG island was completely methylated in the majority of GC cell lines tested (Figure 2B). In addition, bisulfite pyrosequencing revealed high levels of DNA methylation in the GC cell lines, whereas only limited methylation was found in normal stomach from a healthy individual (Figure 2C). We also carried out bisulfite sequencing in selected samples, which confirmed that the CpG sites in this region are extensively methylated in GC cell lines (Figure 2D). In contrast, the majority of CpG sites are unmethylated in normal stomach (Figure 2D).

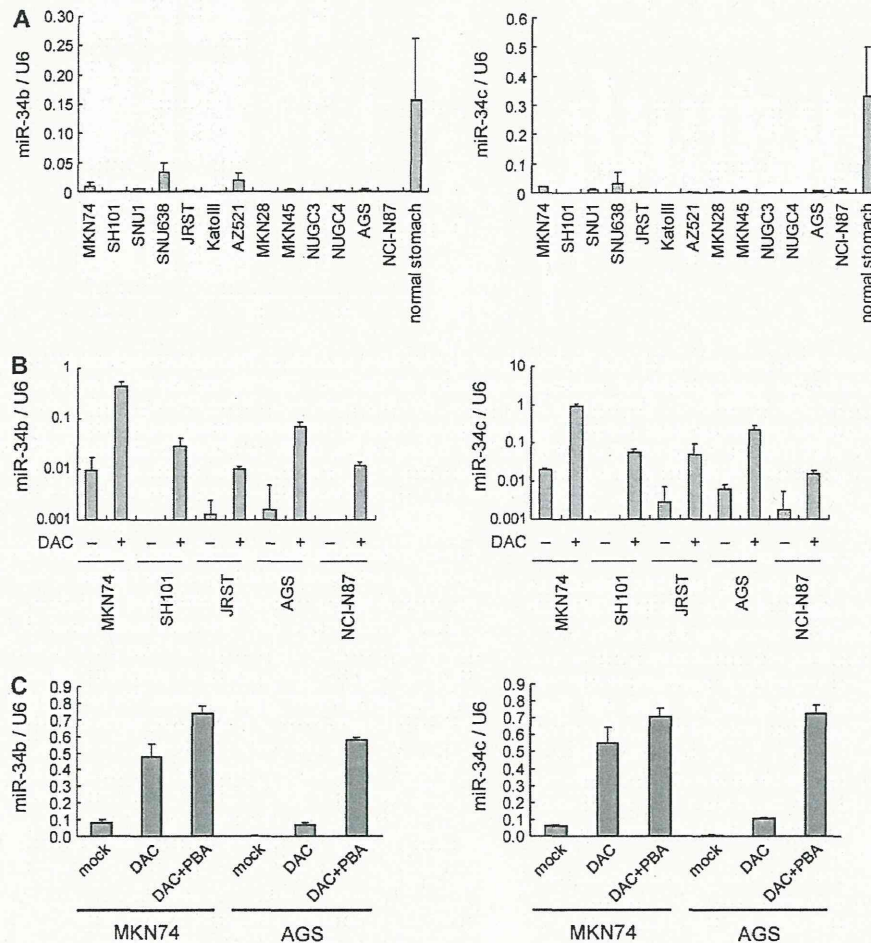


Fig. 1. Analysis of *miR-34b/c* expression in GC cell lines. (A) TaqMan RT-PCR results for *miR-34b* and *miR-34c* in a panel of GC cell lines and normal stomach tissue. Results are normalized to internal U6 snoRNA expression. Shown are the means of three replications; error bars represent standard deviations. (B) TaqMan RT-PCR results for *miR-34b* and *miR-34c* in the indicated GC cell lines, with (+) or without (-) DAC treatment. (C) TaqMan RT-PCR results for *miR-34b* and *miR-34c* in the indicated GC cell lines, with DAC alone or DAC plus PBA or without treatment (mock).

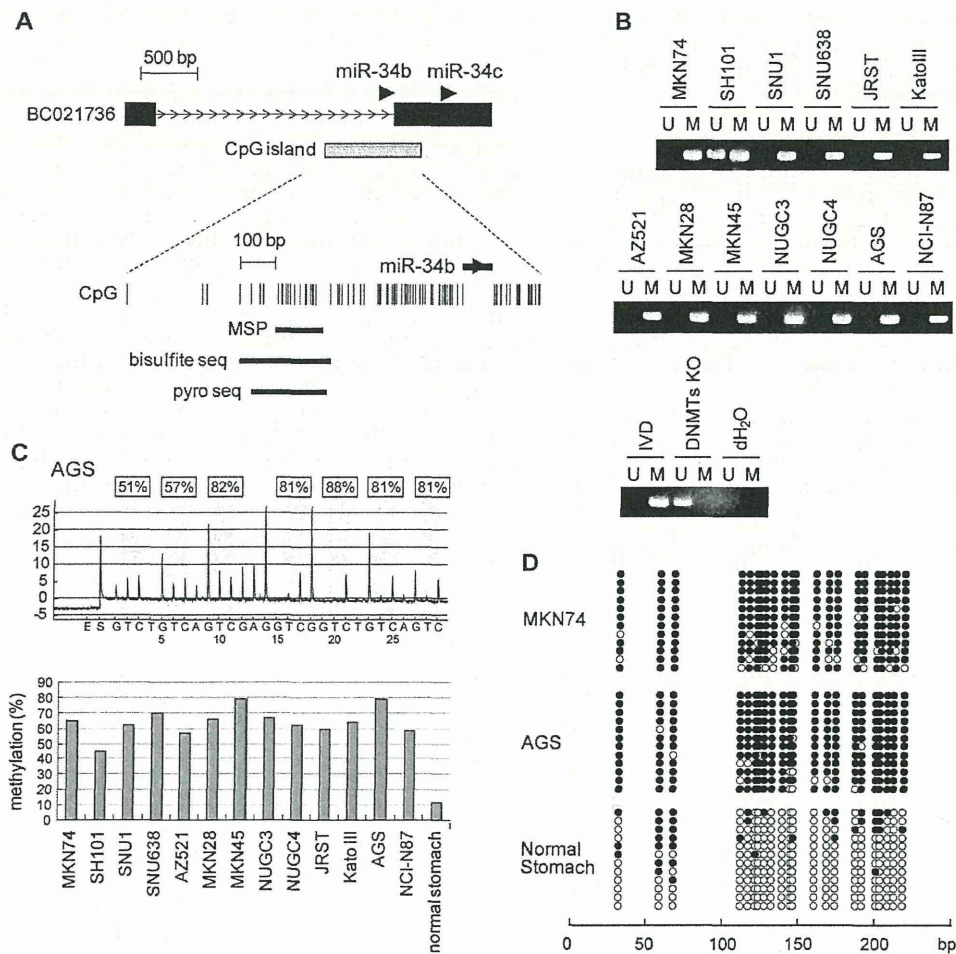


Fig. 2. Methylation analysis of the *miR-34b/c* CpG island in GC cells. (A) Diagram of the *miR-34b/c* CpG island. The regions analyzed using methylation-specific PCR (MSP), bisulfite sequencing and bisulfite pyrosequencing are indicated by bars below the CpG sites. (B) MSP analysis of the *miR-34b/c* CpG island in a set of GC cell lines. *In vitro* methylated DNA (IVD) and DNMT KO cells served as positive and negative controls, respectively. Bands in the 'M' lanes are PCR products obtained with methylation-specific primers and those in the 'U' lanes are products obtained with unmethylated-specific primers. (C) Bisulfite pyrosequencing analysis of *miR-34b/c* in GC cell lines. A representative result in AGS cells is shown above, and the percent methylation at seven CpG sites is indicated on the top. Shown below are the summarized results of bisulfite pyrosequencing in GC cell lines and normal stomach tissue. (D) Bisulfite sequencing of the *miR-34b/c* CpG island in the indicated GC cell lines and normal stomach tissue. Open and filled circles represent unmethylated and methylated CpG sites, respectively.

Functional analysis of *miR-34b/c* in GC cells

To test whether *miR-34b* and *miR-34c* serve as tumor suppressors in GC, we transfected GC cell lines (MKN74, AGS and SNU638) with miR precursor molecules or a negative control and then carried out 3-(4,5-dimethylthiazole-2-yl)-2,5-diphenyl tetrazolium bromide assays. We observed that 48 h after transfection, ectopic expression of *miR-34b* and *miR-34c* had suppressed the growth of all three cell lines (Figure 3A). Real-time RT-PCR analysis revealed that expression of hepatocyte growth factor receptor (MET), cyclin-dependent kinase 4 (CDK4) and cyclin E2 (CCNE2), three well-known targets of *miR-34s*, was suppressed in the transfected cells (8) (Figure 3B). In addition, western blot analysis revealed significant suppression of MET protein (Figure 3C).

To further clarify the effect of the miRNAs, we used oligonucleotide microarrays to assess global changes in the gene expression profile induced by *miR-34b/c* in SNU638 cells. We found that 1113 probe sets were downregulated (>1.5-fold) by ectopic *miR-34b* expression and 3202 were downregulated by ectopic *miR-34c* expression. And because of the high homology between *miR-34b* and *miR-34c*, there was significant overlap between the genes downregulated by the two miRNAs (supplementary Figure 3 and Table 7 are available at

Carcinogenesis Online). Our microarray analysis also revealed that a number of cell cycle-related genes were downregulated by *miR-34b/c*, and gene ontology analysis showed that 'cell cycle phase' genes and 'mitosis' genes were the most enriched among the downregulated genes (supplementary Table 8 is available at *Carcinogenesis Online*). We next searched for significant pathways affected by *miR-34b/c* using the list of downregulated genes. We found that a number of cell cycle-related processes (e.g. M phase, mitosis and the G₂/M transition checkpoint) were affected by *miR-34b/c* in GC cells (supplementary Figure 4 is available at *Carcinogenesis Online*), and downregulation of a representative gene (CCNA2) was confirmed by real-time RT-PCR and western blot analysis (Figure 3B and C).

Finally, using real-time RT-PCR, we observed that cell cycle-related genes (CDK4, CCNE2 and CCNA2) were also downregulated in AGS cells treated with DAC plus PBA, suggesting reexpression of endogenous miRNAs can exert effects similar to those seen with transfection of exogenous miR precursor molecules (Figure 3D).

Analysis of *miR-34b/c* methylation and expression in primary GC

We next analyzed the methylation of the *miR-34b/c* CpG island in a panel of tumor specimens from GC patients. Using bisulfite

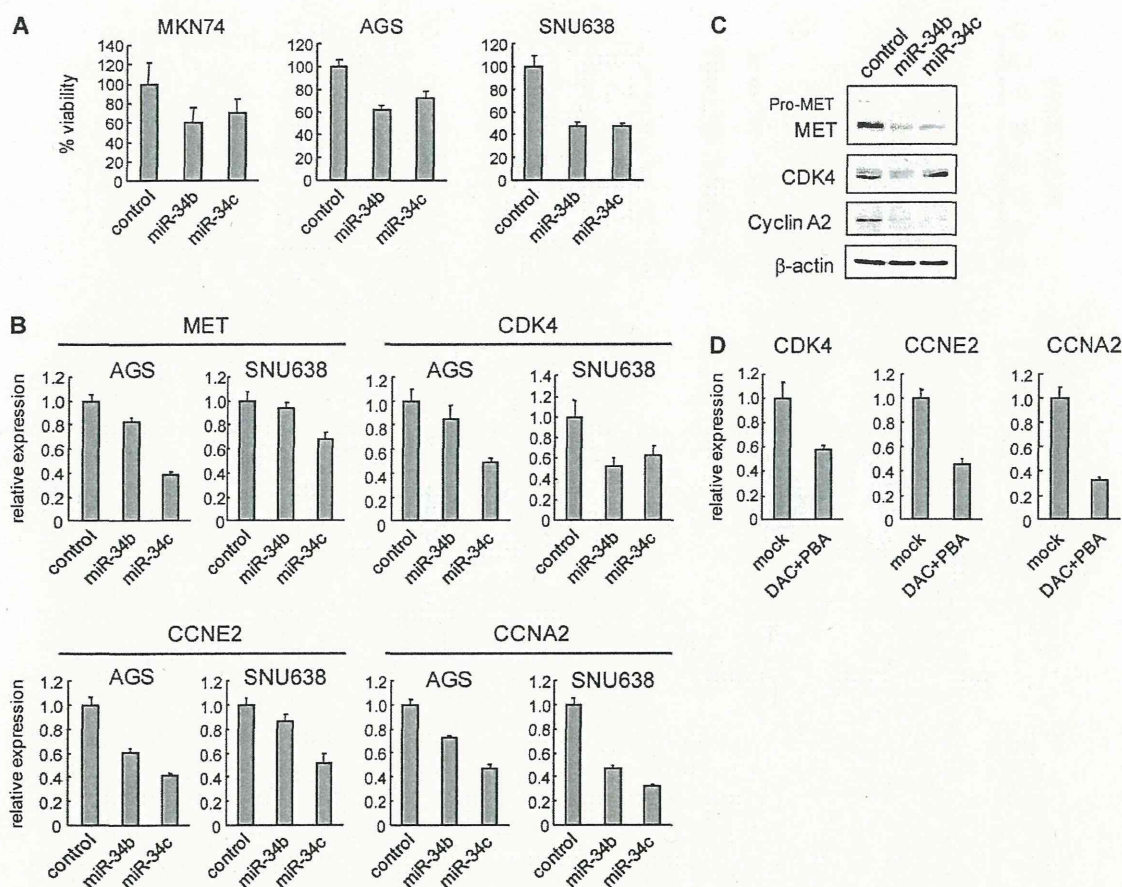


Fig. 3. Functional analysis of *miR-34b/c*. (A) Ectopic expression of *miR-34b/c* suppresses GC cell growth. GC cell lines were transfected with *miR-34b* or *miR-34c* precursor molecules or a negative control. Cell viabilities were determined in 3-(4,5-dimethylthiazole-2-yl)-2,5-diphenyl tetrazolium bromide assays carried out 48 h after transfection. Values were normalized to cells transfected with a negative control. Shown are the means of eight replications; error bars represent standard deviations. (B) Real-time RT-PCR analysis of candidate target genes in the indicated GC cell lines transfected with *miR-34b* or *miR-34c* precursor molecules. Results are shown relative to a value of 1 assigned to cells transfected with a negative control, after normalization to internal 18S ribosomal RNA expression. Shown are the means of three replications; error bars represent standard deviations. (C) Western blot analysis of the gene products downregulated by *miR-34b/c* in SNU638 cells. (D) Real-time RT-PCR analysis in AGS cells treated with or without DAC plus PBA. Results are shown relative to a value of 1 assigned to cells treated with mock, after normalization to internal 18S ribosomal RNA expression.

pyrosequencing, we detected elevated levels of *miR-34b/c* methylation (>15.0%) in 83 of 118 (70.3%) primary GCs tested. In contrast, only limited (<15.0%) methylation was detected in normal gastric mucosa from *H. pylori*-negative healthy individuals, indicating that methylation of the *miR-34b/c* region is a tumor-predominant phenomenon (Figure 4A). We confirmed these results with bisulfite sequencing in selected specimens. Tumor tissue showed a mixture of entirely and partially methylated alleles, as well as unmethylated alleles that probably reflected contamination of the sample by normal cells (Figure 4B). No significant correlation between *miR-34b/c* methylation and clinicopathological characteristics or between p53 mutation and *miR-34b/c* methylation were observed (data not shown).

We then performed TaqMan RT-PCR to assess the expression of *miR-34b/c* in normal gastric mucosae from healthy individuals ($n = 7$) and primary GC tissues harboring *miR-34b/c* methylation ($n = 14$). We found substantial downregulation of *miR-34b/c* expression in the tumor tissues, as compared with normal gastric mucosae (Figure 4C). We also used *in situ* hybridization to assess the spatial distribution of the miRNAs in GC tissues. Using a specific probe, we observed expression of *miR-34b* in a colorectal cancer cell line treated with DAC but not in untreated cells (data not shown). In primary GC specimens, *miR-34b* expression was downregulated in tumor tissues

but was expressed in adjacent non-cancerous tissues (a representative result in supplementary Figure 5, available at *Carcinogenesis* Online).

Elevated methylation of *miR-34b/c* in non-cancerous gastric mucosa

One recent study showed hypermethylation of several miRNA genes in non-cancerous gastric mucosa from GC patients, which suggests the possible involvement of miRNA gene methylation in an epigenetic field defect. We therefore analyzed samples of endoscopically obtained non-cancerous gastric mucosa from 109 GC patients (32 patients with synchronous or metachronous multiple GC and 77 with single GC) and samples of normal gastric mucosa from 85 healthy individuals (78 individuals with *H. pylori* and 7 without). Biopsy specimens were obtained from the gastric body and antrum of each individual, and the average methylation level of the two specimens was determined. Among the healthy individuals, the mean levels of *miR-34b/c* methylation in *H. pylori*-positive and negative gastric mucosae were 20.7% and 7.8%, respectively, suggesting that methylation of *miR-34b/c* is associated with *H. pylori* infection (Figure 4D, Table I). In cancer patients, the mean methylation level in non-cancerous gastric mucosa was 22.7%, which is about the same as in the *H. pylori*-positive healthy individuals. On the other hand, we found that the methylation levels were significantly higher in patients with multiple GC than in those